

Molecular Geometry of Monomeric and Dimeric Yttrium Trichloride from Gas-Phase Electron Diffraction and Quantum Chemical Calculations

Balázs Réffy,[†] Colin J. Marsden,^{*,‡} and Magdolna Hargittai^{*,†}

Structural Chemistry Research Group of the Hungarian Academy of Sciences, Eötvös University, Pf. 32, H-1518 Budapest, Hungary, Laboratoire de Physique Quantique UMR 5626, IRSAMC, Université Paul Sabatier, 118 route de Narbonne, 31062 Toulouse Cedex 04, France

Received: October 8, 2002; In Final Form: January 14, 2003

The molecular geometry of yttrium trichloride has been determined by high-temperature gas-phase electron diffraction. The vapor phase consisted of about 87% monomeric and 13% dimeric species. High-level quantum chemical calculations have also been carried out for both the monomer and dimer of yttrium trichloride, and their geometries, harmonic force fields, and vibrational frequencies have been determined. The monomer YCl_3 molecule was found to be planar (D_{3h} symmetry) both by experiment and by computation. The bond length of YCl_3 from electron diffraction is 2.450(7) (r_g) or 2.422(12) (r_e) Å. It proved remarkably difficult to obtain a converged theoretical prediction for the bond length; large polarization bases are needed, and the published bases accompanying the pseudopotentials used appear to be overcontracted. The SCF method predicts bonds that are too long by some 0.043 Å, whereas the B3LYP method overestimates by about 0.03 Å. The B3PW91 prediction is almost within the experimental uncertainty for r_e . Among the traditional correlated methods, the MP2 distance with an infinitely large basis is probably indistinguishable from the experimental value, given the combined uncertainties, whereas the estimated CCSD(T) result of 2.423(10) Å is astonishingly close to the experimental result. The out-of-plane bending motion for YCl_3 is noticeably anharmonic, with the result that straightforward quantum predictions of its frequency are lower than the value observed in the gas phase at high temperature.

Introduction

The study of molecular potential energy surfaces, which for molecules containing more than a handful of atoms means essentially the molecular structure and harmonic force field, continues to be a major preoccupation for physical chemists. For those who are interested in a qualitative discussion of bonding properties, knowledge of the molecular structure is clearly a prerequisite. For those who like to analyze trends in structural properties, it is obviously necessary for precise and reliable structural data to be available. Though one might imagine that the molecular structures and harmonic force fields of “simple” binary halides such as YCl_3 would have been determined long ago, in fact, the experimental study of such species is deceptively complex. Of the possible experimental methods used for structure determination in the gas phase, electron diffraction (ED) is the only one feasible if monomeric YCl_3 is planar with D_{3h} symmetry, as predicted by simple structural models for a compound of group 3. Although this method is indeed a powerful one, several difficulties arise when it is applied to metal halides. First, because these compounds have very low volatility, high temperatures must be used to produce sufficient vapor pressure. Second, these high temperatures necessarily excite many quanta of the low-frequency bending motions, leading to large shrinkage effects whose description will be challenging if the bending motions are appreciably nonharmonic. Third, the vapor composition is

unlikely to be simple; depending on the temperature and pressure, a fairly complex mixture of monomers, dimers and possibly trimers will be present.¹ It is unrealistic to expect a study based only on experimental ED data to be able to establish both the composition of such a mixture and the structural parameters of its components, especially because the dimer bond lengths may differ only slightly from those in the monomer.

Because there are clearly severe difficulties associated with an experimental study of gaseous YCl_3 , one might be tempted to imagine that a computational approach would be more suitable. In view of the remarkable recent improvements in both computing hardware and theoretical methods, YCl_3 might seem a relatively modest structural challenge to those who prefer a computational approach. Although it is certain that computations are indeed a very powerful tool for the structural chemist, the accuracy provided by standard theoretical methods is in fact often rather disappointing, if one is aiming for errors of only a few thousandths of an ångström or tenths of a degree. For example, we showed a few years ago² that very large polarization bases are necessary for both Mg and Cl to obtain converged bond length predictions for monomeric MgCl_2 , bases far larger than those that could conveniently be applied to the study of the dimer. For atoms that are appreciably heavier than Mg, it is standard practice to use pseudopotentials to represent the core electrons. But the accuracy available for bond lengths is sometimes no better than moderate when pseudopotentials are used. It is now clear that great care must be taken to account for core-polarization effects when atoms toward the left of the Periodic Table, such as Y, are treated.^{1,3}

The conclusion to be drawn from these general remarks is that to obtain the most complete and reliable set of information

* Corresponding authors: E-mail addresses: marsden@irsamc.ups-tlse.fr; hargittaim@ludens.elte.hu.

[†] Eötvös University.

[‡] Université Paul Sabatier.

on the gas-phase structures of metal halides, there are great advantages in combining theoretical and experimental methods. Each approach has its strong points, but these do not coincide. The ED method will yield a precise (and, if vibrational effects are properly treated, accurate) value for the average bond length in a complex mixture, but will not, in general, be able to provide reliable values for the rather subtle differences between monomer and dimer parameters. The computational approach can provide values for these differences, and provided that it can be shown that these are rather insensitive to details of both the basis and theoretical method adopted, one has good reason to suppose that the theoretical structural data can supplement the experiment without degrading it by the introduction of systematic errors. Our earlier experience with similar systems with complicated vapor composition has been encouraging.^{2,4,5} In the present work, we obviously wished to extract as much structural information as possible from the ED experimental method, while using the results of the extensive theoretical computations where that seemed appropriate.

There are several structural analyses of YCl_3 in the literature, though with contradictory results. Selivanov et al.⁶ determined the ν_3 frequency of the monomer in their gas-phase infrared study. So did Perov et al.⁷ in a matrix-isolation experiment. Both of them agree that YCl_3 has a planar, D_{3h} equilibrium molecular structure. Konings et al., however, reported all four wavenumbers in their more recent and detailed paper,⁸ and they deduced that the monomer is pyramidal. Then followed the first ab initio study by Marsden and Smart.⁹ They suggested a different assignment of Konings spectra, supported by their SCF and MP2 calculations which both predicted a D_{3h} geometry for YCl_3 . A recent ab initio study by Solomonik et al. comes to the same conclusion as to the shape of this molecule, together with the other scandium and yttrium halides.¹⁰ Other works also support the planarity of group 3 trihalides; see ScCl_3 ,^{11,12} YBr_3 ,¹³ and YI_3 .¹⁴ At the same time, information about the shapes of the trifluorides ScF_3 and YF_3 is contradictory; details may be found in ref 1.

Dimers of similar molecules have also been investigated, such as Sc_2Cl_6 by Haaland et al. in a combined gas electron diffraction–density functional study¹² and Y_2Br_6 ¹³ and several rare earth halide monomers and dimers, including La_2Cl_6 ,¹⁵ by Kovács.

The geometry of yttrium trichloride was studied by gas-phase electron diffraction in the 1950s by Akishin et al.¹⁶ They also reported a planar structure for the molecule. Because that study was done by the old visual technique, a reinvestigation of the molecule by modern methods is certainly warranted.

Experimental Section

The sample of yttrium trichloride was prepared by dehydration of crystalline $\text{YCl}_3 \cdot 6\text{H}_2\text{O}$ as described in ref 8 and kindly given to us by Dr. R. J. M. Konings of The Netherlands Energy Research Foundation. The combined electron-diffraction and quadrupole mass-spectrometric experiment developed in the Budapest laboratory¹⁷ was used, with the modified EG-100A apparatus¹⁸ and with a radiation-type nozzle system and a molybdenum nozzle. The accelerating voltage was 60 kV. The mass spectra indicated a certain amount of dimeric species in the vapor in addition to monomers. The temperature of the electron diffraction experiment was 1312 K. Four and five plates were used in the analysis taken at 50 and 19 cm camera ranges, respectively. The data intervals were 1.75–14.0 \AA^{-1} (with 0.125 \AA^{-1} steps) and 7.75–35.5 \AA^{-1} (with 0.25 \AA^{-1} steps) at the 50 and 19 cm camera ranges, respectively. Electron scattering

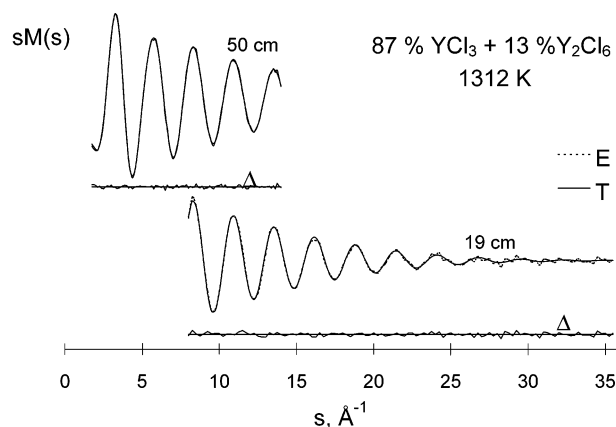


Figure 1. Experimental (E) and calculated (T) molecular intensities and their differences (Δ).

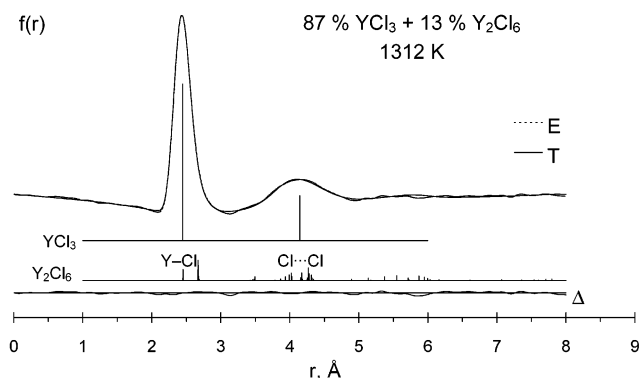


Figure 2. Experimental (E) and calculated (T) radial distributions and their differences (Δ). The vertical bars indicate the relative contribution of different distances.

factors were taken from the literature.¹⁹ Listings of total electron diffraction intensities are given as Supporting Information. The molecular intensity and radial distribution curves are shown in Figures 1 and 2.

Quantum Chemical Calculations

An extensive series of quantum calculations was performed, with the aim of checking the sensitivity of the results to both the size of the basis set and the type of theoretical method employed. Geometries were optimized and vibrational frequencies calculated using many of the standard methods available in the Gaussian98 program:²⁰ SCF, MP2, MP3, MP4DQ, MP4SDQ, MP4SDTQ, CISD, CCSD, CCSD(T), B3LYP, and B3PW91. Analytical methods for obtaining the first and second derivatives of the energy were adopted where feasible. Although for convenience we describe the quantum calculations and the ED analysis in separate sections, it must be understood that there was in fact a constant interplay between them; when the initial quantum calculations appeared to be inadequate, as judged by unacceptable differences between some elements of the computed force field and the results of the ED analysis, more elaborate ones were undertaken to try to uncover the sources of the errors.

A “Stuttgart” “small-core” pseudopotential developed by Preuss and co-workers was always adopted for the Y atom ($Z = 39$).²¹ The associated 8s7p6d basis set contracted to 6s5p3d (11 electrons treated explicitly for the neutral atom ($Z = 39$), in the 4s, 4p, 5s, and 4d atomic orbitals) is large and apparently quite flexible (but see the Results below). Two different treatments were adopted for the Cl atom; initially, a Stuttgart

pseudopotential was employed to treat the 10 core electrons,²² with the associated 4s5p basis contracted to 2s3p for the seven valence electrons, but to verify that this time-saving procedure did not induce errors of any consequence, calculations were also undertaken with the McLean–Chandler all-electron basis²³ for Cl (12s9p contracted to 6s5p, with diffuse s and p functions added, whose exponents were chosen by downward extrapolation, to account for the substantial net negative charge carried by the Cl atoms in YCl₃). These two series of calculations are denoted 1 and 2, respectively. Unless specifically noted otherwise, all the electrons were correlated in series 1 calculations (32 for the monomer, 64 for the dimer), though excitations into the four (eight) highest energy virtual orbitals were excluded for the monomer (dimer). In most of the calculations in series 2, the same number of electrons was correlated as for series 1, though in some cases the core-like 2s and 2p electrons on Cl were also correlated. Excitations into the 16 highest energy virtual orbitals were excluded for the monomer in series 2 calculations.

It was initially anticipated that the role of the calculations would be limited to providing data to support the ED analysis. The most important uses that were envisaged were to help establish the (presumably small) differences in the analogous structural parameters of the monomer and dimer, and to yield force constants from which usefully accurate vibrational amplitudes and shrinkages could be obtained. It appeared that density functional theory would be quite sufficient for these purposes. The polarization space of the s, p basis sets described above was systematically expanded, with exponents roughly optimized for monomeric YCl₃ at the B3LYP level of theory. Basis A contains a single set of d-type functions on Cl (exponent 0.4), whereas two sets are found in basis B (exponents 1.0 and 0.3). Basis C is obtained from B by adding a single set of f-type functions to the Y basis (exponent 0.35), whereas basis D is obtained from C by adding a set of f-type functions to the Cl basis (exponent 0.6). Pure spherical-harmonic representations were adopted throughout. The number of contracted functions for monomeric YCl₃ is therefore 84, 99, 106, and 127 for bases A–D, respectively, in series 1, or 126, 141, 148, and 169 in series 2. The same polarization functions were adopted in series 1 and 2, except where specifically noted otherwise.

The optimized bond length for monomeric YCl₃, obtained at four different levels of theory (SCF, MP2, B3LYP, and B3PW91) and with the four different bases A–D for both series 1 and 2 (32 different combinations), is reported in Table 1, together with bond lengths obtained at higher correlated levels (with basis A only). For reasons that will become clear later, we also present the corresponding harmonic value of the out-of-plane bending frequency ω_2 (a_2'' symmetry). Analysis of these data can be found in the Results. We note that the default (“fine”) grid used with DFT methods in Gaussian98 for numerical integration, with 75 radial shells and 302 angular points per shell, is quite inadequate for the calculation of the lowest vibrational frequency, as the use of the “ultrafine” grid, with 99 radial shells and 590 points per shell, changed the calculated value of ω_2 from 12 to 34 cm⁻¹ (basis A, B3PW91 method, series 1). This ultrafine grid was therefore used for all the calculations of vibrational frequencies reported in this work. We checked that further improvement in the grid size, for example, to 125 radial shells and 770 points per shell, gave insignificant changes to that vibrational frequency.

To probe the anharmonicity of this out-of-plane motion, the puckering potential was calculated with a much larger partially uncontracted basis E'' containing 3f1g polarization functions

TABLE 1: Computed Bond Lengths and Out-of-Plane Bending Frequencies of YCl₃^a

method	A		B		C		D	
	<i>r</i>	ω_2	<i>r</i>	ω_2	<i>r</i>	ω_2	<i>r</i>	ω_2
Series 1								
SCF	2.476	57	2.476	58	2.467	60	2.465	59
B3LYP	2.459	35	2.458	37	2.452	40	2.450	39
B3PW91	2.446	34	2.445	36	2.438	40	2.436	39
MP2	2.456	46	2.452	48	2.428	45	2.417	44
MP3	2.463	50						
MP4DQ	2.466	47						
MP4SDQ	2.464	48					2.427	48
MP4SDTQ	2.465	45						
CISD	2.463	51						
CCSD	2.464	49					2.427	49
CCSD(T)	2.464	47					2.426	46
Series 2								
SCF	2.483	57	2.483	58	2.473	60	2.471	59
B3LYP	2.463	36	2.462	37	2.453	40	2.451	40
B3PW91	2.448	34	2.447	36	2.438	39	2.437	39
MP2	2.462	37	2.460	41	2.433	41	2.422	39
MP3	2.468	43						
MP4DQ	2.468	43						
MP4SDQ	2.469	41						
CCSD	2.469	42						

^a Bond lengths in ångströms, frequencies in cm⁻¹. The molecule is planar, D_{3h} , by all methods. Basis A: single d-type polarization on Cl, none on Y. Basis B: double d-type on Cl, none on Y. Basis C: B plus f-type on Y. Basis D: C plus f-type on Cl. For further details see text. Series 1 and 2 defined in the text.

TABLE 2: Out-of-Plane Puckering Potential^a Computed for YCl₃

puckering angle (deg) ^b	Δr^c	ΔE^d
3	-0.0008	0.360
6	-0.0018	1.372
9	-0.0037	3.400
12	-0.0060	6.212
15	-0.0090	10.118
18	-0.0123	15.316
21	-0.0160	22.134
24	-0.0192	31.071
27	-0.0217	42.889
30	-0.0227	58.651

^a Basis E'', MP4SDQ method. ^b Difference between 90° and the angle between the C₃ axis and a Y–Cl bond. ^c Change in optimized bond length, compared to planar geometry, in ångströms. ^d Increase in energy due to puckering, in kJ/mol.

on Y and 3d1f on Cl, at the MP4SDQ level of theory. The choice of this method and basis is justified in the Supporting Information. The angle between the C₃ axis and the Y–Cl bonds was progressively increased from 90° to 120°, in steps of 3°. The bond length was optimized at each step. We report the change in optimized bond length and the energy increase for each step in Table 2.

D_{2h} symmetry was initially assumed for the Y₂Cl₆ dimer; i.e., each Y atom is bound to two bridging and two terminal Cl atoms, giving a distorted tetrahedral environment about Y, as shown in Figure 3. This assumption was verified by the subsequent calculation of vibrational frequencies, all of which were found to be real at SCF, B3LYP, B3PW91, and MP2 levels of theory, and by our failure to find another competitive true minimum, despite extensive searches. Geometry optimizations were performed at several of the same levels of theory as for the monomer. The resulting structural parameters (four geometrical degrees of freedom) are reported in Table 3 (four levels of theory, four different basis sets, and two series, making 32 different combinations), whereas the harmonic vibrational

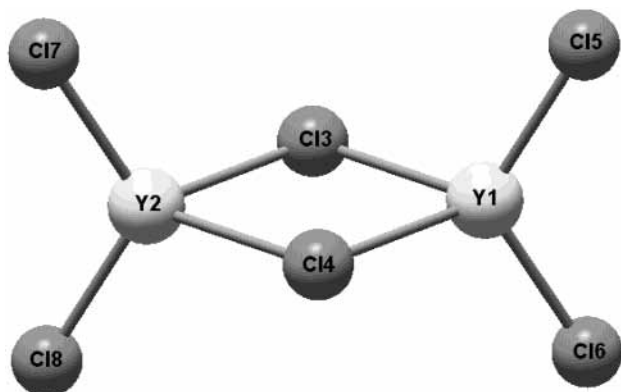


Figure 3. Molecular model and numbering of atoms in Y_2Cl_6 .

wavenumbers together with the ones for the monomer may be found in Table 4.

The puckering potential of the central four-membered ring of the Y_2Cl_6 dimer was studied at the B3PW91 level of theory. The ring was folded about the axis containing the two bridging Cl atoms and passing through the ring center. The angle between the two YCl_2 (bridging) planes was fixed at values ranging from 10 to 70°, in 10° steps, and the remaining six geometrical degrees of freedom were optimized. Results are reported in Table 5; note that the symmetry of the dimer is lowered from D_{2h} to C_{2v} on puckering.

Normal Coordinate Analysis

A normal coordinate analysis was performed using the program ASYM20²⁴ for both monomeric and dimeric molecules. Experimental vibrational wavenumbers are available for the monomer in the literature, except for the symmetric stretching mode (see Table 4). We have computed the vibrational frequencies and force fields for both monomeric and dimeric species at several different levels of approximation. The vibrational characteristics of the yttrium trichloride dimer are reported here for the first time.

Monomeric yttrium trichloride was found to be planar (D_{3h} symmetry) at all levels of computation. Accordingly, it has six normal vibrational modes: $\Gamma_{\text{vib}}(YCl_3) = A_1' + A_2'' + 2E'$. The halogen-bridged dimer (D_{2h}) has 18 normal modes of vibration: $\Gamma_{\text{vib}}(Y_2Cl_6) = 4A_g + A_u + 2B_{1g} + 2B_{1u} + 2B_{2g} + 3B_{2u} + B_{3g} + 3B_u$. The computed force-field parameters of both species in the symmetry coordinate representation are given as Supporting Information.

The latest gas-phase infrared spectroscopic wavenumbers⁸ were used for the monomer, with the revised assignment suggested by Marsden and Smart,⁹ which is also in agreement with the present study (see Table 4). Vibrational amplitudes, given in Table 6, were obtained in two ways. In one case, the missing experimental symmetric stretching frequency ν_1 of the monomer was estimated from the computed frequencies by scaling the computed stretching force constants to the experimental antisymmetric stretching wavenumber in the literature (ν_3 , 370 cm^{-1} , refs 6 and 8). Then the normal coordinate analysis was performed on the basis of the three experimental frequencies and the estimated value of the symmetric stretching mode. In another set of calculations, only the calculated frequencies were used.

As there is no experimental vibrational information on the dimer, the computed frequencies and force field (basis D, B3PW91 method) were used in the normal coordinate analysis. Here, again, two different routes were followed. In one, the scale

factor calculated for the monomer stretching force constant (0.913) was also applied to the force constants associated with the stretching modes of the dimer, and the vibrational amplitudes were calculated using this scaled force field. In the other approach, the computed force constants were used without any adjustment. It appeared that the amplitudes calculated from the directly computed force field agreed better with the experimental values than did those obtained from the scaled force field, and so the former were used in the subsequent ED analysis.

The dimer is a very floppy system, as witnessed by the large number of low frequencies, the lowest being found at just 17 cm^{-1} . This deformation (ring puckering, b_{2u} symmetry) mode has a profound influence on the vibrational amplitudes calculated for the longest nonbonded distances. In our dynamic electron diffraction analysis (vide infra), therefore, the so-called “framework amplitudes” were used, as they are not influenced by this deformation motion. They were calculated by excluding the lowest frequency from the normal coordinate analysis. The resulting amplitudes of the dimer are also given in Table 6.

Structure Analysis

With more than 10% of dimeric molecules present in the vapor, certain constraints have to be applied in the ED analysis. First of all, the *difference* between the two types of dimer Y–Cl bond lengths (terminal and bridging, see Figure 3), and the *difference* of the dimer terminal distance from that of the monomer, were taken from the computations. Although the physical meaning of the geometrical parameters coming from computation and from electron diffraction is not the same,^{1,25} these changes more-or-less cancel when we take *differences* between two similar parameters rather than their absolute values. However, our earlier experience has shown that even this supposition has to be scrutinized carefully.⁴ We were reassured by noting that the computed values of these differences between different Y–Cl distances vary only very slightly with either the basis or the theoretical method used for their calculation (see Tables 1 and 3). We decided to adopt the values computed at the B3PW91 level of theory with basis D.

Initially, a conventional “static” ED analysis was carried out, allowing for the presence of both monomeric and dimeric molecules. The relative abundances of monomers and dimers were consistent with the mass spectrum. In this analysis, each species is represented by one geometrical arrangement, which is an average or static model. The monomer Y–Cl bond length, the monomer $Cl \cdots Cl$ distance, the vapor composition, and the dimer bond angles (Cl_b-Y-Cl_b and Cl_t-Y-Cl_t , Cl_b referring to the bridging and Cl_t to the terminal chlorine atoms, respectively; see Figure 3) were refined as independent parameters. The amplitudes of all three bond lengths were refined together in a group, with a constant difference applied. The asymmetry parameters, κ , for the bond distances were also tied together and refined.

For floppy molecules with large-amplitude vibrations, such static models have certain limitations. For metal di- and trihalides, whose apparent symmetry is lower than their equilibrium symmetry due to shrinkage effects, dynamic models should provide a better (more realistic) description. In such a dynamic model, the large-amplitude motion is approximated by a series of rigid geometries that change gradually along the large-amplitude coordinate. The proportion of these different “conformers” present is determined according to their relative energy, by a Boltzmann factor.

In the present work, both the monomer and the dimer can be described using such an approach. The puckering potential of

TABLE 3: Computed Structural Parameters of Y_2Cl_6 ^a

method and basis	$r(Y-Cl_t)$	$r(Y-Cl_b)$	$\angle Cl_t-Y-Cl_t$	$\angle Cl_b-Y-Cl_b$	$\Delta[r(Y-Cl)_m - r(Y-Cl)_t]$	$\Delta[r(Y-Cl)_b - r(Y-Cl)_t]$
Series 1						
SCF A	2.466	2.690	118.4	81.9	0.011	0.224
SCF B	2.467	2.690	118.4	82.4	0.009	0.223
SCF C	2.458	2.681	118.7	82.4	0.009	0.223
SCF D	2.456	2.680	118.7	82.2	0.009	0.224
MP2 A	2.444	2.647	118.0	83.5	0.012	0.203
MP2 B	2.441	2.639	118.5	83.7	0.011	0.198
MP2 C	2.417	2.609	118.5	84.1	0.011	0.192
MP2 D	2.407	2.596	118.6	84.0	0.010	0.189
B3LYP A	2.449	2.665	116.9	83.7	0.011	0.216
B3LYP B	2.447	2.662	116.3	84.4	0.010	0.214
B3LYP C	2.441	2.655	116.7	84.2	0.010	0.214
B3LYP D	2.438	2.652	116.8	84.0	0.011	0.213
B3PW91 A	2.435	2.648	116.2	84.1	0.011	0.212
B3PW91 B	2.434	2.646	116.2	84.4	0.011	0.212
B3PW91 C	2.428	2.639	116.7	84.2	0.010	0.211
B3PW91 D	2.426	2.637	116.7	84.0	0.010	0.211
Series 2						
SCF A	2.473	2.702	118.4	82.3	0.010	0.229
SCF B	2.473	2.700	118.4	82.8	0.010	0.227
SCF C	2.463	2.688	118.6	82.5	0.010	0.225
SCF D	2.462	2.687	118.7	82.5	0.009	0.225
MP2 A	2.449	2.656	117.6	84.2	0.013	0.207
MP2 B	2.448	2.650	117.7	84.3	0.012	0.202
MP2 C	2.422	2.618	117.8	84.2	0.011	0.196
MP2 D	2.412	2.604	117.9	84.1	0.010	0.192
B3LYP A	2.451	2.671	116.6	84.1	0.012	0.220
B3LYP B	2.450	2.670	116.1	84.6	0.012	0.219
B3LYP C	2.441	2.658	116.5	84.1	0.011	0.217
B3LYP D	2.440	2.657	116.6	84.1	0.011	0.217
B3PW91 A	2.436	2.653	116.6	84.2	0.012	0.217
B3PW91 B	2.436	2.652	116.2	84.6	0.011	0.216
B3PW91 C	2.427	2.640	116.6	84.1	0.011	0.213
B3PW91 D	2.425	2.638	117.0	83.9	0.011	0.213

^a Bond lengths in ångströms, angles in degrees. Basis A: single d-type polarization on Cl, none on Y. Basis B: double d-type on Cl, none on Y. Basis C: B plus f-type on Y. Basis D: C plus f-type on Cl. For further details see text. Series 1 and 2 defined in the text.

TABLE 4: Vibrational Frequencies (cm^{-1}) and Infrared Intensities (km/mol) of YCl_3 and Y_2Cl_6 from Computation and Infrared Spectroscopy

	YCl_3						
	experimental				computed		
	Perov ^a (ref 7)	Selivanov ^b (ref 6)	Konings ^b (ref 8)	suggested reassignment of ref 8 ^d	Marsden, Smart (ref 9)	Solomonik (ref 10)	this work ^c
A_1' (ν_1)			378 ^e		330	340	332
A_2'' (ν_2)			78 ^f	58.6	52	54	39 ^g
E' (ν_3)	351	370	359 ^e	370	393	399 ^h	387 (288)
E' (ν_4)			58.6 ^f	78	78	79 ^h	81 (44)
Y_2Cl_6							
computed, this work ^c							
A_g	370	B_{1g}	384	B_{2g}	217	B_{3g}	68
A_g	262	B_{1g}	45	B_{2g}	66	B_{3u}	355 (184)
A_g	121	B_{1u}	267 (69)	B_{2u}	389 (249)	B_{3u}	257 (130)
A_g	63	B_{1u}	51 (23)	B_{2u}	97 (3)	B_{3u}	79 (9)
A_u	34			B_{2u}	17 (1)		

^a In Xe matrix. ^b In the gas phase. ^c From B3PW91/basis D computations. Infrared intensities, when different from zero, are indicated in parentheses. ^d Suggestion by us and also by refs 9 and 10. ^e Probably wrong assignment, based on unnecessary deconvolution of the band at 370 cm^{-1} , which should correspond solely to the antisymmetric stretching frequency; see text. ^f Most probably wrong assignment, the ν_2 and ν_4 frequencies are interchanged; see text. ^g Our best estimate of this frequency at the MP4SDQ level with the basis F is 52 cm^{-1} ; for details about the anharmonicity of the out-of-plane vibration, see text. ^h The table in the paper indicates these frequencies as "exp", due to a probable misprint.

the central four-membered ring of the dimer, and the out-of-plane, or puckering, potential of the monomer, can both be obtained from quantum chemical calculations and used as constraints in the ED analysis. However, such a model for the monomer presupposes its shape. Because one of the principal questions of our study concerned the shape (symmetry) of monomeric YCl_3 , a different approach was initially adopted.

The geometry of the dimer was described by the dynamic model with a series of conformers, but the monomer was treated by an average model with two parameters, the Y-Cl bond length and the Cl...Cl nonbonded distance. From these two distances, the experimental shrinkage can be calculated and compared with the value derived from the normal coordinate analysis. With this approach we can hope to obtain reliable results for the shape

TABLE 5: Geometrical Parameters and Ring Puckering Potential for Dimeric Yttrium Trichloride from Computation^a

	\angle_{puck} (deg)							
	0	10	20	30	40	50	60	70
Y ₁ -Cl ₅	2.435	2.433	2.434	2.433	2.431	2.429	2.429	2.429
Y ₁ -Cl ₆	2.435	2.436	2.435	2.436	2.436	2.434	2.431	2.426
Y ₁ -Cl ₃	2.647	2.648	2.650	2.652	2.656	2.664	2.676	2.693
$\angle X-Y_1-Cl_5$ ^b	121.7	120.9	120.8	119.6	119.1	120.3	123.5	127.6
$\angle X-Y_1-Cl_6$ ^b	121.7	123.4	123.3	123.3	124.2	124.0	121.8	119.2
$\angle Cl_3-Y_1-Cl_4$	84.0	83.9	83.5	82.8	81.7	80.2	78.1	75.8
ΔE	0	0.49	2.55	6.40	12.56	22.62	39.57	67.00

^a Bond lengths in ångströms, angles in degrees, and energies in kJ/mol. ^b X is the center of the four-membered ring.

TABLE 6: Calculated Vibrational Amplitudes (Å) for YCl₃ and Y₂Cl₆ from Normal Coordinate Analysis

	I ^a	II ^b
Monomer		
$l(Y-Cl)$	0.095	0.099
$l(Cl\cdots Cl)$	0.319	0.321
Dimer ^c		
$l(Y_1-Cl_5)$	0.100	0.096
$l(Y_1-Cl_3)$	0.151	0.144
$l(Y_1\cdots Y_2)$	0.197	0.203
$l(Cl_3\cdots Cl_4)$	0.208	0.216
$l(Cl_3\cdots Cl_5)$	0.464	0.461
$l(Cl_5\cdots Cl_6)$	0.340	0.338
$l(Cl_5\cdots Cl_7)$	0.422	0.425
$l(Cl_5\cdots Cl_8)$	0.540	0.543

^a Scaled according to the monomer experimental frequencies; see text. ^b Based on the computed force field without scaling. ^c For numbering of atoms, see Figure 3. In both cases only frame vibrations considered in the dimer; see text.

and symmetry of the monomer molecule. In a third series of refinements, a dynamic model was adopted for both the monomer and dimer. With this model, we remove the reliance on the harmonic treatment of the principal shrinkage effects in the monomer. If the fit to the ED data in this third approach is similar to that for the second, we may deduce that the quantum chemical calculations and the experimental ED data are providing consistent information about the shape and out-of-plane bending potential for the monomer.

The geometries of the different static conformers with different ring-flapping angles for the dimer were independently optimized in the computations (B3PW91 method), and the changes in their geometries were constrained in the dynamic analysis, as were the relative abundances of the conformers. The differences between the monomer and two types of dimer bond lengths were also taken from the computation and constrained. The monomer Y-Cl vibrational amplitude was refined, and the two Y-Cl dimer amplitudes were tied to that with fixed offsets, but the amplitudes of all the remaining dimer distances were taken from the normal coordinate analysis without change. The asymmetry parameters of the bond distances in the dimer conformers of the preferred model were kept at zero.

Results

Quantum Chemical Calculations. First we summarize here the extensive series of quantum computations that we undertook on YCl₃ monomers and dimers. The details of these computations and their discussion can be found among the Supporting Information (<http://pubs.acs.org>) under the title "Results of the Computations". Next we proceed to comment on the ED structural analysis. More general remarks about YCl₃, comparing its structure to those of related systems, may be found in the Conclusions.

Several interesting points emerge from a careful study of Table 1 that presents results for monomeric YCl₃. First, we note that the bond lengths are always *decreased* by the effects of electron correlation, whether these are incorporated explicitly at the MP2 level or implicitly by density functional theory. Because conventional covalent bonds are systematically *lengthened* by correlation effects, we infer that the most appropriate zeroth-order description of the Y-Cl bonds will take Y³⁺ and Cl⁻ as the interacting entities; in other words, the ionic character is more influential than the covalent. Second, although the optimized bond length systematically decreases as the quality of the basis is improved, the rate of change depends crucially on the method employed. The two versions of density functional theory are the least sensitive to basis quality, as is often found, and scarcely differ from each other in this respect. The SCF results vary just a little more quickly than the DFT, but the MP2 variation is 4 times as great. Because the DFT results appear to be essentially converged for basis D, we chose this combination as our "workhorse" for the subsequent force field calculations. The bond length obtained with the B3PW91 functional is systematically about 0.015 Å shorter than the B3LYP value, and in better agreement with the experimental ED value ($r_e = 2.422(12)$ Å; see below).

The out-of-plane bending mode is of vital significance for the theoretical calculation of the shrinkage effect of YCl₃, and because a proper treatment of the shrinkage effect is essential if the ED experiment is to be able to determine whether YCl₃ is planar or not, the importance of these calculated wavenumbers is considerable. The SCF value is about 60, the MP2 result about 45 or 40, depending on whether a pseudopotential is or is not used for Cl, and the DFT value is about 40 cm⁻¹. These data appear to be roughly converged with the size of basis. Because the experimental gas-phase result is 58.6 cm⁻¹,⁸ the "better" quantum values (those obtained at correlated levels of theory) are clearly less accurate than the more elementary (approximate) SCF results. This observation is particularly worrying, because the shrinkage effect deduced from the ED analysis is consistent with a frequency of about 70 cm⁻¹. It is also surprising to note that a value of 52 cm⁻¹ was reported in the earlier ab initio (MP2) study by Marsden and Smart,⁹ that value is apparently less inaccurate than the current results. Now larger, more flexible bases were used in the present study, both for the s, p and polarization components (the bases adopted earlier⁹ are of (5s5p4d)/[3s3p2d] and (3s3p1d)/[2s2p1d] quality for Y and Cl, respectively). It is therefore a little disconcerting to find that the better bases produce poorer agreement with experiment. These observations led us to undertake systematic examinations both of different computational methods and of extensions to the polarization basis sets, to attempt to reach a converged ab initio prediction of the harmonic vibrational frequency for the out-of-plane bending motion.

The optimized Y-Cl bond length, together with the harmonic frequency of ω_2 , calculated at progressively more rigorous levels

of theory ranging from MP2 to CCSD(T) are also presented in Table 1. Basis A was adopted for this study. Despite its small size, we felt that it would be sufficient to indicate the variation in the properties of interest as the correlation treatment is improved. Although the changes in bond length and out-of-plane bending frequency with theoretical method are not large, they are not negligible. It is clear that the MP2 bond distance is shorter than those obtained at higher levels of theory, both for series 1 and 2. The MP4SDQ results are close to those at the more rigorous CCSD level, and the influence of triple excitations on the bond length is small, though they do decrease the out-of-plane bending frequency slightly. It also appears that the effect of triple excitations is overestimated using perturbation theory. To verify the first two of these points, the larger basis D was used: the resulting MP4SDQ, CCSD, and CCSD(T) optimized bond lengths and out-of-plane bending frequencies are reported in Table 1. Following these results, we decided to use the largest bases feasible at the MP4SDQ level of theory for our “final” values.

The polarization bases were then roughly optimized for both Y and Cl (series 1) at the MP2 level. Details are provided in the Supporting Information. Up to four sets of d-type functions were added to the Cl basis, using the even-tempered approach, followed by up to four sets of f-type functions on Y. It is noteworthy that a single set of d functions on Cl gives a slightly larger geometrical effect than the presumably almost saturated quadruple set, even though in energy terms the single set is inadequate. The energetic and geometrical changes do not move in parallel. It is also noticeable that the geometrical influence of f functions on Y is slightly larger than that of d functions on Cl, even though their energetic effect is much smaller.

Second-order polarization functions were then considered (f-type on Cl, g-type on Y), still adopting the pseudopotential for Cl, at the MP2 level of theory. As these also produced changes to the energy and bond length that are far from negligible, a few additional tests were performed with g-type functions on Cl and h-type on Y. Surprisingly large geometrical changes were observed. These results are rather depressing; the largest basis considered (4d2f2g/Cl and 4f3g1h/Y) contains 312 contracted functions, and its use at levels of theory beyond MP2 becomes quite expensive. Yet it seems that convergence on the bond length has not yet been attained. Moreover, the predicted bond length of 2.375 Å is now significantly different from the r_e value of 2.422(12) Å obtained from the ED experiment (see below).

Attention was then paid to the valence parts of the Y and Cl bases. It became clear that the recommended contraction scheme for the d-type function on Y²¹ is too severe, leading to predicted bond lengths that are noticeably too short, and strong coupling effects between the contractions of the Y and Cl bases were observed. Bases E, E', E'', F, and G and their performance are described in the Supporting Information.

We now attempt to provide a “best theoretical estimate” of the bond length. The CCSD(T) method leads to bond lengths that are marginally shorter, by some two or three thousandths of an ångström, than the MP4SDQ values. As the T1 statistic²⁶ for YCl₃ is only 0.010, the CCSD(T) method should be extremely reliable. The MP4SDQ/basis G bond length of 2.431 Å therefore implies an estimated CCSD(T) value with basis G of 2.428 Å, which is quite consistent with the ED result (see below) of 2.422(12) Å for r_e , being within the experimental uncertainty. But convergence with basis for the bond length at the MP4SDQ level has probably not been attained with basis G; extension of the polarization space beyond basis G might produce a reduction in bond length of at least 0.005 Å, with an

uncertainty at least as large as that. We have no information about the possible inadequacies in the pseudopotential used for Y, and an additional uncertainty of at least 0.005 Å seems likely. Our best estimate is therefore 2.423(10) Å, and it must be admitted that the assessment of the uncertainty is a very subjective exercise. The agreement between experiment and theory therefore seems to be remarkable, as the difference between the two values is only one thousandth of an ångström. Though that level of agreement should not, of course, be taken literally, as the uncertainties in both values are an order of magnitude greater than the difference, it is nonetheless very satisfying. The estimated MP2 extrapolated bond length will be 2.415(10) Å, also within the experimental uncertainty.

The out-of-plane bending frequency was then calculated, with bases E–G at different levels of theory, to see whether the discrepancy between experiment and theory had diminished. The calculated out-of-plane harmonic bending frequency appears to have almost converged, to about 50 cm⁻¹, at the MP4SDQ/G level of theory, yet it is still below the experimental gas-phase value of 59 cm⁻¹ and also lower than the value of about 70 cm⁻¹ implied by the shrinkage observed in the ED experiment. Although a discrepancy of some 10 or 20 cm⁻¹ may seem trivial, a change of this magnitude has a large influence on the calculated shrinkage effect for the Cl···Cl distance, and thus on the Cl–Y–Cl angle deduced in the electron diffraction analysis.

In a further attempt to uncover the source of this discrepancy, we decided to calculate the out-of-plane bending potential for YCl₃. If this potential has a positive anharmonicity, i.e., if it can be expressed as

$$\Delta E = a(\Delta\theta)^2 + b(\Delta\theta)^4$$

where ΔE represents the energy change due to puckering, $\Delta\theta$ is the change in the angle between the C₃ axis and a Y–Cl bond, and both a and b are positive constants, the effective vibrational frequency in the gas phase will be higher than the fundamental frequency (recall that the ED experiment was performed at 1312 K, and the gas-phase IR spectrum was also obtained at high temperatures). Our results are presented in Table 2; the MP4SDQ method was used with basis E''. Analysis of these data shows that the anharmonicity in this motion is indeed positive, as the energy increase for a puckering angle of 15° (27°) is larger than that for 3° by a factor of 28.1 (119.1), rather than by 25 (81) for a purely harmonic potential. The vibrational levels for this potential were obtained by solution of the one-dimensional vibrational Schrödinger equation. The energy difference between adjacent levels increases from 51 cm⁻¹ for the fundamental transition to 54 cm⁻¹ for $\nu = 10$, 57 cm⁻¹ for $\nu = 20$, and 60 cm⁻¹ for $\nu = 30$. The total vibrational energy in this mode is 556, 1115, and 1701 cm⁻¹ for $\nu = 10$, 20, and 30, respectively. At 1312 K, the thermal energy kT corresponds to 912 cm⁻¹. It therefore appears that the effective (average) vibrational frequency for this out-of-plane bending motion at the temperature of the ED experiment will be larger than its harmonic value, by the order of 10%. Though these considerations do not quantitatively resolve the problems associated with the comparison of computed, directly observed (gas-phase IR), and indirectly inferred (ED shrinkage) values of the vibrational frequency, they do at least substantially diminish the discrepancies noted above.

Finally, we considered whether the use of a pseudopotential on Cl was an acceptable approximation in the quantum calculations. Our various tests (see the Supporting Information) lead us to believe that pseudopotentials on Cl can be used

TABLE 7: Geometrical Parameters of YCl_3 and Y_2Cl_6 from Electron Diffraction^a

	$r_g, \text{\AA}$	l	κ
Static Model ^b			
YCl_3			
Y–Cl	2.445 ± 0.007^c	0.090 ± 0.003	$5.57 \times 10^{-5} \pm 9.83 \times 10^{-6}$
Cl \cdots Cl	4.191 ± 0.031	0.333 ± 0.020	
$\angle_{\text{a}}\text{Cl}–\text{Y}–\text{Cl}$	117.3 ± 1.8		
Y_2Cl_6			
Y–Cl _t	2.435 ± 0.007^c	0.090 ± 0.003	$5.57 \times 10^{-5} \pm 9.83 \times 10^{-6}$
Y–Cl _b	2.654 ± 0.020^c	0.130 ± 0.019	$3.32 \times 10^{-4} \pm 2.73 \times 10^{-4}$
Y \cdots Y	3.874 ± 0.029		
$\angle_{\text{a}}\text{Cl}_b–\text{Y}–\text{Cl}_b$	87.3 ± 1.1		
$\angle_{\text{a}}\text{Cl}_t–\text{Y}–\text{Cl}_t$	117.1 ± 2.3		
α^d	10.0		
monomer (%)	84.0 ± 4.0		
R (%) ^e	5.00		
Dynamic Model for Dimer Only ^f (Preferred Model)			
YCl_3			
Y–Cl	2.450 ± 0.007^c	0.091 ± 0.002	$7.25 \times 10^{-5} \pm 9.05 \times 10^{-6}$
Y–Cl (r_e) ^g	2.422 ± 0.012		
Cl \cdots Cl	4.169 ± 0.025	0.316 ± 0.010	
$\angle_{\text{a}}\text{Cl}–\text{Y}–\text{Cl}$	115.9 ± 1.3		
δ^h	0.075 ± 0.033		
Y_2Cl_6			
Y–Cl _t	2.439 ± 0.008^c	0.092 ± 0.002	
Y–Cl _b	2.659 ± 0.002^c	0.141 ± 0.010	
Y \cdots Y	3.950 ± 0.042		
$\angle\text{Cl}_b–\text{Y}–\text{Cl}_b$	84.0^i		
$\angle\text{Cl}_t–\text{Y}–\text{Cl}_t$	116.6^i		
monomer (%)	87.0 ± 4.5		
R (%) ^e	4.98		
Dynamic Model for Monomer and Dimer ^j			
YCl_3			
Y–Cl	2.448 ± 0.007^c	0.0088 ± 0.002	$4.72 \times 10^{-5} \pm 9.05 \times 10^{-6}$
Y–Cl (r_e) ^g	2.422 ± 0.012		
Cl \cdots Cl	4.258 ± 0.025	0.318 ± 0.010	
$\angle\text{Cl}–\text{Y}–\text{Cl}$	120.0		
Y_2Cl_6			
Y–Cl _t	2.438 ± 0.008^c	0.092 ± 0.002	$4.72 \times 10^{-5} \pm 9.05 \times 10^{-6}$
Y–Cl _b	2.657 ± 0.0017^c	0.141 ± 0.010	$1.04 \times 10^{-4} \pm 9.05 \times 10^{-6}$
Y \cdots Y	3.948 ± 0.042		
$\angle\text{Cl}_b–\text{Y}–\text{Cl}_b$	84.0^i		
$\angle\text{Cl}_t–\text{Y}–\text{Cl}_t$	116.6^i		
monomer (%)	87.8 ± 4.5		
R (%) ^e	5.63		

^a Bond lengths, shrinkage and vibrational amplitudes in ångströms, asymmetry parameter (κ) in cubic ångströms, angles in degrees. Error limits are estimated total errors, including systematic errors and the effect of constraint used in the refinement. $\sigma_i = (2\sigma_{LS}^2 + (cp)^2 + \Delta^2)^{1/2}$, where σ_{LS} is the standard deviation of the least-squares refinement, p is the parameter, c is 0.002 for distances, 0.02 for amplitudes, and Δ is the effect of constraints. ^b The geometry for both molecules corresponds to lower symmetry (C_{3v} and C_{2v} for the monomer and dimer, respectively) thermal-average structures. ^c Differences of dimer terminal and monomer and the two types of dimer bond distances constrained at the B3PW91 (basis D) values. ^d Apparent puckering angle of the dimer. Refined with a trial and error method. ^e Goodness of fit. ^f The geometry given for the monomer is a thermally averaged C_{3v} -symmetry structure, whereas for the dimer it corresponds to a D_{2h} -symmetry structure. The differences between the “bent conformer” parameters of the dimer were taken from the computation and kept unchanged (see text for details). ^g Equilibrium bond length estimated by a Morse-type correction, $r_e^M = r_g - (3al^2)/2$ (a is the Morse constant and l is the mean-square vibrational amplitude). ^h Experimental shrinkage; $\delta = \sqrt{3}r(\text{Y}–\text{Cl}) - r(\text{Cl}\cdots\text{Cl})$. ⁱ Taken from the B3PW91 (basis D) computation and not refined. ^j The geometry given for the monomer and the dimer corresponds to a D_{3h} and D_{2h} -symmetry structure, respectively. The changes in all parameters for the “bent conformers” were taken from the computation and kept unchanged (see text for details).

without inducing significant error, and that an all-electron basis is in fact more demanding when the size of the polarization space is considered.

Table 3 shows that changes to the dimer structural parameters produced by improvements to the basis set are similar to those for the monomer. For obvious reasons, the dimer could not be studied in such detail, or with such large bases, as the monomer. It is important to note that the Y–Cl terminal bonds in the dimer are consistently about 0.01 Å shorter than those in the monomer (from the 32 sets of results in Table 1, this difference ranges from 0.009 to 0.013 Å, whereas if we concentrate on the largest basis, it ranges only from 0.009 to 0.011 Å). The Y–Cl bridging

bonds are appreciably longer than those in the monomer, by some 0.2 Å; the range of this difference is 0.040 Å over the 32 results in Table 1, or 0.031 Å if the SCF results are excluded. The difference is largest at the SCF level (0.22–0.23 Å) and smallest for MP2 calculations (0.19–0.20 Å). For a given method, it decreases slowly as the basis is improved. The angles within the four-membered ring are larger at Cl than at Y, by some 13°, whereas the terminal bonds make an angle at Y that is about 8° larger than the tetrahedral value. These angular parameters vary slightly with the theoretical method, but by less than 3° over the 32 sets of results in Table 3.

A few results obtained with larger bases are available for the

dimer. It is noticeable (and reassuring) that the MP2 values of the two differences in bond length become closer to the DFT results that were adopted for the ED analysis. Similarly, the MP2 values for the angles at Y are 118.4 (117.9) and 84.7° (84.6) with basis E (E'), whereas the B3PW91 results are 116.7 (116.6) and 84.0° (84.2) with basis D (E).

Electron Diffraction. The results of the electron diffraction analysis are given in Table 7. The bond length determined by ED is of course a thermal-average value, and as such has a different physical meaning from the computed values discussed above, which are equilibrium distances.^{1,25} Comparison of these two types of results is meaningful only if we carry out vibrational corrections to the ED values.²⁷ If Morse-type anharmonicity is assumed for the Y–Cl bonds, the estimated experimental r_e distance is 2.422(12) Å, which agrees remarkably well with the estimated ab initio (CCSD(T)) value of 2.423(10) Å discussed above. Although the B3PW91 prediction is just about within the uncertainty of the experimental r_e , the B3LYP result is less good, and the SCF distance is clearly too long.

The ED analysis has been carried out with three different approaches. The simplest and least accurate is the so-called static model, described earlier. A much better description is the dynamic model that treats floppy molecules, especially the dimer, as a series of rigid “conformers” whose rigid geometries change gradually along the large-amplitude coordinate. Our second model uses this approach for the dimer but the monomer is still treated as a static average structure (see Table 7). The reason for this choice of model is that we wanted to see if the shape of this molecule could be determined by ED alone; but by applying a dynamic model for the monomer as well, we would have already presupposed its shape. This mixed model was found to be the best description of our system. The bond angle determined for the monomer by this approach is a thermal-average value, involving the so-called shrinkage effect. From this shrinkage, 0.075 ± 0.033 Å, the puckering frequency can be estimated as 72 cm^{-1} . The rather large uncertainty of the shrinkage is due to the large uncertainty of the Cl···Cl distance. Taking this uncertainty into consideration, the lower limit estimated for ν_2 is 54 cm^{-1} , whereas the upper limit, 141 cm^{-1} , is obviously too large. Considering the large uncertainty, our estimated 72 cm^{-1} puckering frequency agrees satisfactorily with the value determined by gas-phase infrared spectroscopy, 59 cm^{-1} .⁸ At the same time, the calculated shrinkage, corresponding to the B3PW91 frequency of 39 cm^{-1} , is 0.178 Å, obviously much larger than the ED value (see our discussion about the problems associated with the computation of this frequency). Because the ED shrinkage is smaller than the value calculated from the computed frequencies, the planarity of the molecule is safely established.

The third approach of the ED analysis uses a dynamical model for both the monomer and the dimer. In this case the computed puckering potential was used for both molecules together with the differences in the geometrical parameters of the different “puckered” conformers as constraints. The agreement for this approach is slightly worse than for the partly static partly dynamical model, but still acceptable. There could be a number of reasons for the somewhat poorer agreement; the large number of constraints applied or the fact that the vibrational amplitudes for all conformers were assumed to be equal to that of the calculated higher symmetry species, just to mention two.

Conclusions

Group 2 metal dihalides have intriguing shapes, as both linear and bent geometries are found.^{1,28} It is well-known that their

shapes cannot be reliably predicted by simple models that are normally successful in main-group chemistry, such as the VSEPR rules²⁹ or Walsh diagrams.³⁰ All the barium dihalides, CaF₂, SrF₂, and SrCl₂ are bent at equilibrium, though in some cases the bending potential is almost flat. The present authors favor the idea that core polarization of the central atom leads to bent rather than linear geometries if it is large and sufficiently polarizable, though other authors note that hybridization effects cannot strictly be separated from core polarization.^{3a} The shape of the lanthanide trihalides poses a similar problem; experimental and computational information on this topic is rather contradictory (see ref 1, for example). Yttrium trihalides invite interesting comparisons with both of these groups.

It is instructive to consider the ionic radii and dipole polarizabilities of the different cations, in conjunction with the structural preferences of their halides. The ionic radius of Y³⁺ (1.04 Å) falls between those of Mg²⁺ (0.71 Å) and Ca²⁺ (1.14 Å).³¹ The bond lengths of monomeric MgCl₂, YCl₃, and CaCl₂ obviously follow the same trend: 2.179(5),² 2.450(7), and 2.483(6)³² Å. The calculated polarizabilities of the cations, in atomic units, are Mg²⁺, 0.46; Ca²⁺, 3.2; Sr²⁺, 5.2; Ba²⁺, 13.4; Al³⁺, 0.26; Sc³⁺, 2.1; Y³⁺, 4.0; and La³⁺, 7.6. These are SCF values and are believed to be converged to the number of digits given. The extra charge on a group 3 cation means that it is always less polarizable than its neighbor in group 2, by a factor that is typically about 0.6. However, the group 3 cations are also smaller than their group 2 neighbors. But geometrical factors ensure that the energy gain due to pyramidalization of a planar MX₃ molecule is significantly less than that due to the bending of a linear M'X₂ system, if the distances and cation polarizabilities are the same. These rather qualitative remarks rationalize the planarity of YCl₃, the pyramidal equilibrium geometry reported for some lanthanum trihalides,¹ and the observation of nonlinearity for group 2 halides at the Ca/Sr periods, depending on the anion.

Acknowledgment. C.J.M. thanks Dr. N. Halberstadt for the anharmonic vibrational calculation of the out-of-plane bending mode. He is also grateful to the CINES, Montpellier, France, for generous provision of computing facilities (project pqt1073), and to Dr. P. R. Taylor for helpful discussions. We thank Mária Kolonits for her experimental work and Ms. Judit Molnár for her participation in the initial stages of the analysis. Support of the Hungarian National Research Fund (OTKA T037978) is gratefully acknowledged.

Supporting Information Available: Total electron diffraction molecular intensities at two different camera ranges, the computed force-field parameters of YCl₃ and Y₂Cl₆ in the symmetry coordinate representation, and the detailed discussion of the quantum chemical computations. This material is available free of charge via the Internet at <http://pubs.acs.org>.

References and Notes

- (1) Hargittai, M. *Chem. Rev.* **2000**, *100*, 2233.
- (2) Molnár, J.; Marsden, C. J.; Hargittai, M. *J. Phys. Chem.* **1995**, *99*, 9062.
- (3) (a) Kaupp, M.; Schleyer, P. v. R.; Stoll, H.; Preuss, H. *J. Am. Chem. Soc.* **1991**, *113*, 6012. (b) Hassett, D. M.; Marsden, C. J. *J. Mol. Struct.* **1995**, *346*, 249.
- (4) Réffy, B.; Kolonits, M.; Hargittai, M. *J. Mol. Struct.* **1998**, *445*, 139.
- (5) Réffy, B.; Kolonits, M.; Schulz, A.; Klapötke, T. M.; Hargittai, M. *J. Am. Chem. Soc.* **2000**, *122*, 3127.
- (6) Selivanov, G. K.; Sekachev, Yu. N.; Maltsev, A. A. *Zh. Fiz. Khim.* **1973**, *47*, 2182.

- (7) Perov, P. L.; Nedjak, S. V.; Maltsev, A. A. *Vestn. Mosk. University, Ser. 2., Khim.* **1975**, *16*, 281.
- (8) Konings, R. J. M.; Booiij, A. S. *J. Mol. Struct.* **1992**, *271*, 183.
- (9) Marsden, C. J.; Smart, B. A. *Ast. J. Chem.* **1993**, *46*, 749.
- (10) Solomonik, V. G.; Marochko, O. Yu. *Russ. J. Phys. Chem.* **2000**, *74*, 2094.
- (11) Jolly, C. A.; Marynick, D. S. *Inorg. Chem.* **1989**, *28*, 2893.
- (12) Haaland, A.; Martinsen, K.-G.; Shorokhov, D. J.; Girichev, G. V.; Sokolov, V. I. *J. Chem. Soc., Dalton Trans.* **1998**, *17*, 2787.
- (13) Kovács, A. *J. Mol. Struct.* **1999**, *482–483*, 403.
- (14) Groen, P.; Kovács, A.; Hargittai, M. Manuscript in preparation.
- (15) Kovács, A. *Chem. Phys. Lett.* **2000**, *319*, 238.
- (16) Akishin, P. A.; Naumov, V. A.; Tatevskii, V. M. *Kristallografiya* **1959**, *4*, 194.
- (17) Hargittai, I.; Tremmel, J.; Kolonits, M. *Hung. Sci. Instrum.* **1980**, *50*, 31; Hargittai, I.; Bohatka, S.; Tremmel, J.; Berecz, I. *Hung. Sci. Instrum.* **1980**, *50*, 51.
- (18) Tremmel, J.; Hargittai, I. *J. Phys. E* **1985**, *18*, 148.
- (19) Ross, A. W.; Fink, M.; Hilderbrandt, R.; Wang, J.; Smith, V. H., Jr. In *International Tables for Crystallography, C*; Wilson, A. J. C., Ed.; Kluwer: Dordrecht, 1995; pp 245–338.
- (20) Frisch, M. J.; Trucks, G. W.; Schlegel, H. B.; Scuseria, G. E.; Robb, M. A.; Cheeseman, J. R.; Zakrzewski, V. G.; Montgomery, J. A., Jr.; Stratmann, R. E.; Burant, J. C.; Dapprich, S.; Millam, J. M.; Daniels, A. D.; Kudin, K. N.; Strain, M. C.; Farkas, O.; Tomasi, J.; Barone, V.; Cossi, M.; Cammi, R.; Mennucci, B.; Pomelli, C.; Adamo, C.; Clifford, S.; Ochterski, J.; Petersson, G. A.; Ayala, P. Y.; Cui, Q.; Morokuma, K.; Malick, D. K.; Rabuck, A. D.; Raghavachari, K.; Foresman, J. B.; Cioslowski, J.; Ortiz, J. V.; Stefanov, B. B.; Liu, G.; Liashenko, A.; Piskorz, P.; Komaromi, I.; Gomperts, R.; Martin, R. L.; Fox, D. J.; Keith, T.; Al-Laham, M. A.; Peng, C. Y.; Nanayakkara, A.; Gonzalez, C.; Challacombe, M.; Gill, P. M. W.; Johnson, B.; Chen, W.; Wong, M. W.; Andres, J. L.; Gonzalez, C.; Head-Gordon, M.; Replogle, E. S.; Pople, J. A. *Gaussian 98*, Revision A.6; Gaussian, Inc.: Pittsburgh, PA, 1998.
- (21) Andrae, D.; Haeussermann, U.; Dolg, M.; Stoll, H.; Preuss, H. *Theor. Chim. Acta* **1990**, *77*, 123.
- (22) Bergner, A.; Dolg, M.; Kuechle, W.; Stoll, H.; Preuss, H. *Mol. Phys.* **1993**, *80*, 1431.
- (23) McLean, A. D.; Chandler, G. S. *J. Chem. Phys.* **1980**, *72*, 5639.
- (24) Hedberg, L.; Mills, I. M. *J. Mol. Spectrosc.* **1993**, *160*, 117.
- (25) Hargittai, M.; Hargittai, I. *Int. J. Quantum Chem.* **1992**, *44*, 1057.
- (26) Lee, T. J.; Taylor, P. R. *Int. J. Quantum Chem. Symp.* **1989**, *23*, 199.
- (27) Kuchitsu, K. *Bull. Chem. Soc. Jpn.* **1967**, *40*, 505.
- (28) Hargittai, M. *Coord. Chem. Rev.* **1988**, *91*, 35.
- (29) Gillespie, R. J.; Hargittai, I. *The VSEPR Model of Molecular Geometry*; Allyn and Bacon: Boston, 1991.
- (30) Walsh, A. D. *J. Chem. Soc.* **1953**, 2266.
- (31) Shannon, R. D. *Acta Crystallogr.* **1976**, *A32*, 751.
- (32) Vajda, E.; Hargittai, M.; Hargittai, I.; Tremmel, J.; Brunvoll, J. *Inorg. Chem.* **1987**, *26*, 1171.